Magnetic Stars, 2011, pp. 295 – 302

First Observational Evidences for the Presence of Active, Localized Magnetic Structures in White Dwarfs

Valyavin G.[1], **Wade G. A.**[2], **Bagnulo S.**[3], **Antonyuk K.**[4], **Plachinda S.**[4], **Clark D. M.**[1], **Fox Machado L.**[1], **Alvarez M.**[1], **Lopez J. M.**[1], **Hiriart D.**[1], **Han I.**[5], **Jeon Y.–B.**[5], **Zharikov S. V.**[1], **Zurita C.**[6,7], **Mujica R.**[8], **Shulyak D.**[9], **Burlakova T.**[10]

[1] Observatorio Astronómico Nacional SPM, Instituto de Astronomía, Universidad Nacional Autónoma de México, Ensenada, BC, México
[2] Physics Department, Royal Military College of Canada, Kingston, Ontario, Canada
[3] Armagh Observatory, Northern Ireland
[4] Crimean Astrophysical Observatory, Nauchny, Crimea, Ukraine
[5] Korea Astronomy and Space Science Institute, Youseong–Gu, Daejeon, Republic of Korea
[6] Instituto de Astrofísica de Canarias, La Laguna, Tenerife, Spain
[7] Departamento de Astrofísica, Universidad de La Laguna, La Laguna, Tenerife, Spain
[8] Instituto Nacional de Astrofísica, Óptica y Electroníca, Tonantzintla, Pueblo, México
[9] Astrophysics, Georg–August–University, Göttingen, Germany
[10] Special Astrophysical Observatory, Nizhny Arkhyz, Russia

Abstract. The magnetic white dwarf WD 1953–011 demonstrates the presence of two–component magnetic field geometry in photosphere. The geometry consists of a weak, large–scale component, and a strong, localized component (magnetic “spot”). The localized component of the field is derived from variable due to the star’s rotation circular polarization and intensity spectra. The flux from WD 1953–011 is also variable with rotation in the V–band filter. This variability can be explained by the presence of a dark spot having a magnetic nature, analogous to sunspots. Motivated by this idea, and using all available observations of WD 1953–011 we examine the possible physical relationships between the suggested dark spot and the strong–field magnetic structure recently identified on the surface of this star. Comparing the rotationally–modulated flux with the variable spectral observables related to the magnetic “spot” we establish their physical relationship. We discuss this result in the frame of the first observational evidences for the presence of active magnetic structures in magnetic white dwarfs.

Key words: stars: individual: WD 1953–011 – stars: magnetic fields – stars: white dwarfs

1 Introduction

WD 1953–011 can be described by the low–field ($B \sim 90$ kG) global and strong–field ($B \sim 500$ kG) localized components, or a “magnetic spot” (Maxted et al., 2000; Valyavin et al., 2008). The presence of the spot (or “tube”, as suggested by Valyavin et al. (2008) seems strange for the isolated white dwarfs due to the fact that their convective–free envelopes make difficult the generation magnetic tubes by analogy to sunspots. Nevertheless, an examination of the idea about the magnetic activity in degenerate stars looks interesting.

If our idea about the magnetic tube in WD 1953–011 is correct, we may expect some other observational effects related to the magnetic spot. For example, according to the basic properties of magnetic fields in stars (for instance, Parker, 1979), and by analogy to sunspots, such localized fields may have a significant impact on the pressure–temperature balance in the photospheres of stars. This may produce a temperature difference between the strong–field area and other parts of the stellar surface. As a result we may expect the rotationally–modulated photometric variability of WD 1953–011. For the same reasons such fields might be unstable and exhibit secular drifts over the stellar surface.

In this context, we point out that a significant photometric variability of WD 1953–011 has also been established (Wade et al., 2003; Brinkworth et al., 2005). Indirectly, this suggests a physical relationship between the dark and magnetic spots, and their possible secular migration. However, previous spectroscopy and available photometry were obtained at different epochs, making it impossible to study this relationship in detail. An examination of these problems is the goal of the current study, based on additional *simultaneous* photometric and spectroscopic observations of WD 1953–011. In this presentation we briefly present the results of these observations and speculatively discuss it. A more sophisticated analysis of the data will be presented later in a special paper which is now under consideration in the Astrophysical Journal (Valyavin et al., 2011).

2 Observations

The main portion of the simultaneous spectral and photometric observations of WD 1953–011 were carried out at the Crimean Astrophysical Observatory (CRAO, Ukraine) during several observing nights between July and August 2007. The low resolution long–slit spectrograph of the 2.6 m telescope ZTSh and the UBVR CCD photometer at the 1.25 m telescope AZT–11 were used in the observations at CRAO. The spectrograph used is a standard instrument intended for low–resolution spectroscopy, and is described by Doroshenko et al. (2008). The spectrograph was used to obtain the spectra of the Hβ region with the grating of 1200 gv/mm providing a wavelength coverage of 4330 Å − 5330 Å. With a slit width of $3''$, the spectral resolving power was about 3.8 Å ($R = 1300$).

The photometric observations were carried out with the Ritchey–Chretien AZT–11 telescope ($D = 1.25$ m; $F = 16$ m). The KAF–1001E CCD–camera (Finger Lakes Instrumentation company), with pixel size $24 \times 24\,\mu$m, frame size 1k×1k pixels, and a standard Johnson V–band filter were used in these observations.

These observations were also supported by a few observing runs during May–June, 2009, with the 2.1–m telescope at the Observatorio Astronómico Nacional (Mexico: OAN SPM). With this instrument we obtained an additional series of spectra of WD 1953–011 using the moderate dispersion echelle spectrograph REOSC with a resolving power of about 17000. The instrument is described in detail by Levine & Chakrabarty (1994, see also the website of the OAN SPM: www.astrossp.unam.mx/indexspm.html). A series of additional photometric observations was also obtained with the standard CCD photometers at the 0.84 and 1.5–m telescopes at SMP (see section “instruments” www.astrossp.unam.mx/indexspm.html). In this study we used the REOSC in the low resolution regime (binnig the spectral material to a resolution of about $R = 3000$).

Standard observational techniques and data reduction were used. In order to analyse the observations of WD 1953–011 in combination with the observations of previous authors (Wade et al., 2003; Brinkworth et al., 2005; Valyavin et al., 2008), all the observational and data processing steps were made similar to those described by those authors.

3 Measurements

In this section we describe the measurements necessary for the analysis of our data. Due to the specific field morphology of WD 1953–011 we begin with some qualitative explanations on the observables we used.

According to previous studies, the magnetic field of WD 1953–011 consists of two distinct components — a low–field global dipole + quadrupole component (Valyavin et al., 2008) superimposed with the localized strong–field area (Maxted et al., 2000). The low–field (~ 100 kG) component of the degenerate was discovered spectroscopically by Koester et al. (1998) via the analysis of the Zeeman pattern in the Hα core. The strong–field "spot" was detected by Maxted et al. (2000) via the observations of additional strong-field Zeeman features in the Hα wings. Both patterns are variable due to the star's rotation, and can be measured independently in high–resolution spectroscopy. Together with the variable flux, these are the most important observables.

Due to the low spectral resolution and S/N of our current spectral observations, (in contrast to that which we used in our previous studies of this degenerate with the 8–m telescope at VLT) here we are unable to provide a robust analysis of the star's global magnetic field revealed in the cores of Balmer lines. However, the strong–field ≈ 0.5 MG magnetic spot can be effectively studied in terms of residual intensities and equivalent widths of the Balmer lines.

The Balmer line profiles in the spectrum of WD 1953–011 vary due to the strong–field magnetic spot. The central intensity r_c of the line cores, and the equivalent widths EW of the lines, correlate strongly with the intensity of the strong–field Zeeman features which are found in the wings of the Balmer lines (for example, see Valyavin et al., 2008, and Fig. 3 therein: the two satellite features are at ± 10 Å around the Hα core). This correlation (the higher the intensity of the features, the weaker r_c and EW, see Fig. 3 in Valyavin et al., 2008) is due to the fact that the spot, which appears periodically on the visible disc due to rotation, significantly redistributes the Hα flux according to its projected area. Taking these arguments into account, we conclude that the minimum of r_c and EW of the Balmer lines corresponds to those moments (or close to those moments), when the strong–field magnetic area is projected towards the observer. The minimum projection of the strong–field area corresponds to the deepest central intensities and largest equivalent widths of the Balmer lines. Due to this, in this paper we use r_c and EW of the star's Balmer spectral lines as the main observables to examine the rotational modulation of the strong–field area, and to compare with the flux variability.

At the same time it is important to note that both the observables r_c and EW are also sensitive to thermal effects at the star's surface and this may introduce some uncertainties in our analysis. However, an empirical examination of our previous, high signal–to–noise spectropolarimetric observations of this star with the VLT made it possible to accept the above assumption as a good first–guess approximation. The analysis of rotationally modulated circular polarization in the Hα wings also supports this assumption, revealing a direct empirical relationship between the amplitudes of circular polarization attributed to the strong–field area and r_c/EW (the higher the circular polarization the lower r_c and EW).

3.1 Spectroscopic Measurements

Taking the above arguments into account we measured the EW and r_c of the Hβ spectral line in the observations with ZTSH and Hα in all other cases. In order to minimize the selection effects due to the use of different telescopes, spectrographs and different spectral lines, all the measurements within individual groups of observations with a given instrument (and spectral line) were normalized by their mean values, averaged over a full rotational cycle of the star. Thus, hereinafter, when mentioning r_c and EW we assume their normalized values. This normalization makes it possible to consider all measurements from different spectral lines together. In this study we also use the measurements from the spectral material obtained in the previous studies with the Anglo–Australian 4–m telescope AAT (Maxted et al., 2000), from the 8–m European telescope and 6–m Russian telescope (Valyavin et al., 2008).

3.2 Photometric Measurements of WD 1953–011

The V–band CCD photometric observations were carried out in the standard manner. As the comparison stars we used the targets, earlier used by Brinkworth et al. (2005). Calibrating the measured fluxes from WD 1953–011 by the fluxes from the standard stars we finally obtained a series of m_V values in stellar magnitudes at each of the individual short–duration (a few minutes) exposures. The characteristic uncertainty of the measurements is about 0.02 stellar magnitudes.

4 Results

4.1 Revising the Rotation Period

The new observables (m_V, r_c, and EW) obtained for WD 1953–011 from photometry and spectroscopy together with the photometric data from Brinkworth et al. (2005) make it possible to revise the degenerate's rotation period on a time base of about 10 years. All the observables used are variable with the star's rotation.

To determine the rotation period we applied the Lafler–Kinman method (Lafler & Kinman, 1965), as modified by V. Goransky (2004, private communication). The power spectra of variation of the observables are presented in Fig. 1. The first plot (from top to bottom) presents the periodogram of m_V obtained from our photometric observations. The second plot is the periodogram obtained from our photometric observations together with those, obtained by Brinkworth et al. (2005). The third plot illustrates the power spectrum of the normalized Hα and Hβ equivalent widths. The fourth plot is the power spectrum of the normalized residual intensity of the Hα and Hβ lines obtained from all the available spectroscopic observations of WD 1953–011. As can be seen, all the spectra exhibit a single strong peak at the frequency of about 0.69 day^{-1} ($P \approx 1.45$ days).

A detailed study of the periodograms has shown that the most significant and sinusoidal signal common to all observables corresponds to the period of $P = 1.441788(6)$ days. This period is very close to $P = 1.441769$ days found by Brinkworth et al. (2005) from their photometry. Due to this agreement, here we choose this period for phasing all the data with the following ephemeris (for which JD 0 corresponds to the maximum of the light variation):

$$\mathrm{JD} = 2,454,329.872 + 1.441788(6)\, E$$

4.2 Phase–Resolved Photometry Against Zeeman Spectroscopy

In Fig. 2 we illustrate the phase variations of the photometric magnitude (the upper two panels on the figure), equivalent widths of the Balmer lines (the third panel from top) and the residual intensity r_c of the lines. All the data are phased with the ephemeris described above. The lower two plots present the phase variation of the degenerate's global surface magnetic field (B_G: mean field modulus integrated over the disc) with the same ephemeris, and the projected fractional area S of the strong–field area on the disc (given in percent of the full disc area). These data are taken from Valyavin et al. (2008) and re–phased with the current ephemeris. The two vertical dashed lines in Fig. 2 correspond to those phases ($\phi \approx 0.5, 1.5$) when the star exhibits the minimum brightness, and therefore the maximum projection of the dark area onto the disc.

As can be seen from Fig. 2, the spectroscopic observable r_c also tends to have the smallest values at the phases of the light minimum. According to the above explanations this suggests a

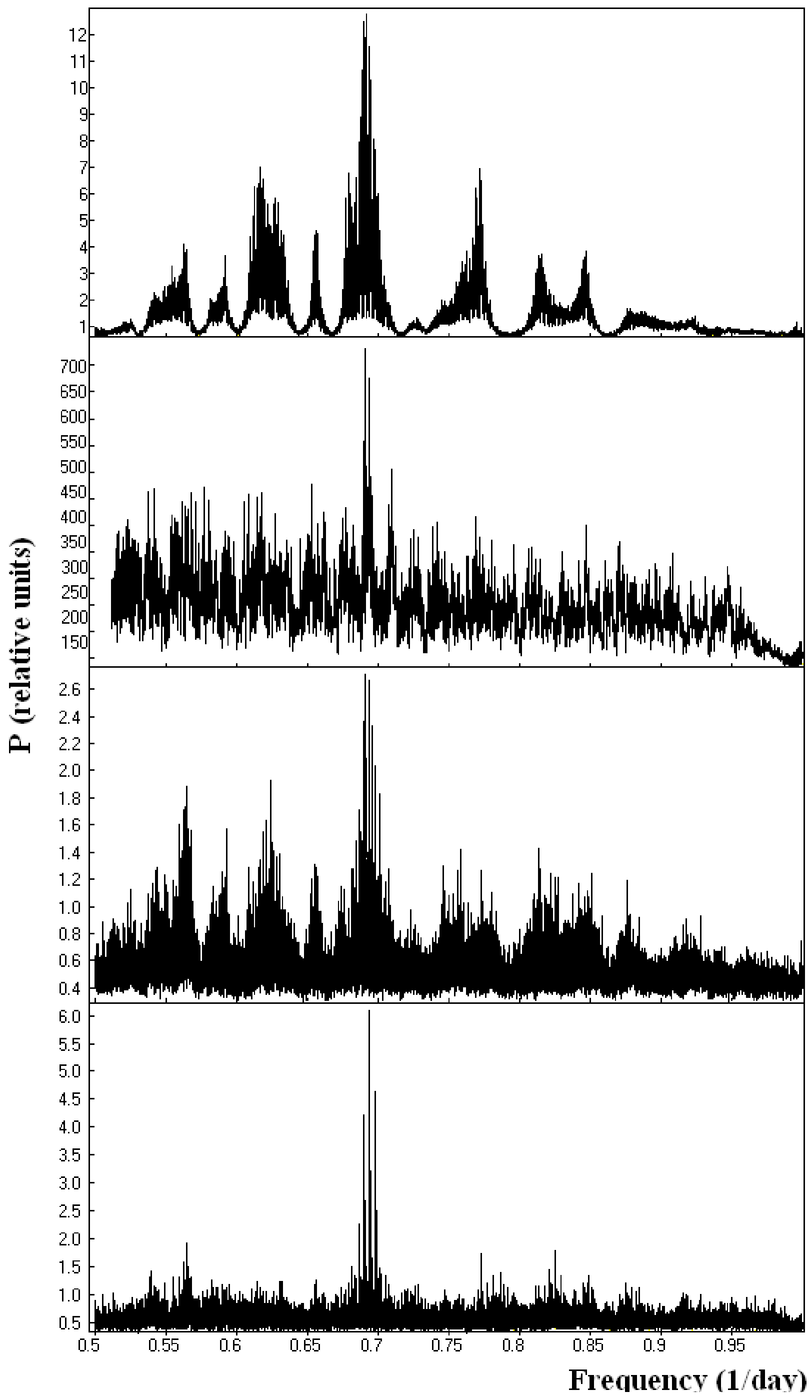

Figure 1: Power spectra of the variation of (from top to bottom): 1 — stellar V–magnitude of WD 1953–011 obtained from our (discussed in this paper) observations; 2 — stellar V–magnitude of WD 1953–011 obtained from our observations together with those obtained by Brinkworth et al. (2005); 3 — normalized Hα and Hβ equivalent widths obtained from all available spectroscopic observations of WD 1953–011 (i. e. from the observations discussed in this paper, from the data of Maxted et al. (2000), and from our previous observations presented by Valyavin et al. (2008); 4 — normalized residual intensities of the Hα and Hβ lines obtained from all the available spectroscopic observations of the degenerate.

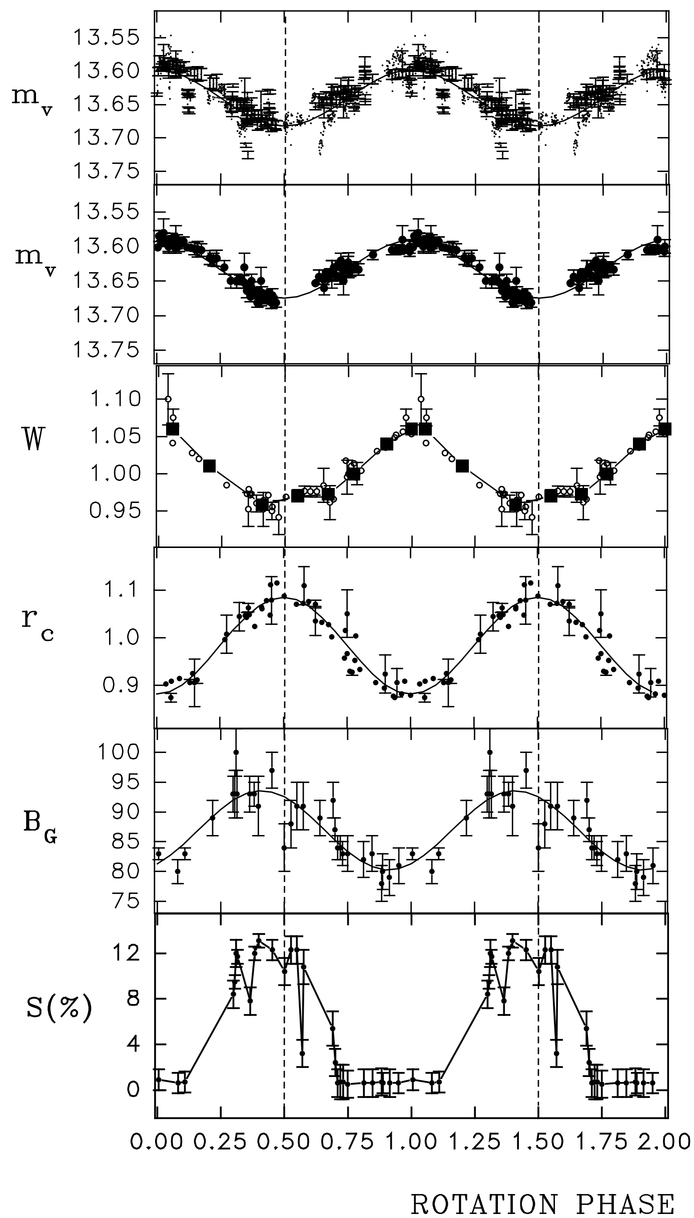

Figure 2: Phase variations with rotation period $P = 1.441788(6)$ days of (from top to bottom): 1 — stellar V–magnitude of WD 1953–011 obtained from our observations together with those obtained by Brinkworth et al. (2005); 2 — stellar V–magnitude of the degenerate obtained from our observations only; 3 — normalized Hα and Hβ equivalent widths obtained from all available spectroscopic observations of WD 1953–011 (i. e. from the observations discussed in this paper, from data of Maxted et al. (2000), and from our previous observations presented by Valyavin et al. (2008)); 4 — normalized residual intensities of the Hα and Hβ lines obtained from all available spectroscopic observations of the degenerate; 5 — global magnetic field of the degenerate; 6 — the projected fractional area of the strong–field area on the disc (the data are taken from Valyavin et al. (2008) and given in percent of the full disc square). The solid sinusoidal lines at plots 1, 2, 4, 5 (from top to bottom) are least–square fits of the data. The solid squares at the middle plot 3 are the averaged data in bins. The two vertical solid lines pass through phases 0.5, 1.5. These phases correspond to the minimum light energy from the star and maximum projection of the magnetic spot to the line of sight.

direct relationship between the dark area and strong–field spot. However, in comparison with the behaviour of the residual intensity, the variation of equivalent width demonstrates a non–sinusoidal shape with its absolute minimum shifted by $\Delta\phi \approx -0.05$ relative to the phase of the light minimum. Phased results of direct measurements of the projected area S (for details, see subsection 4.2 and Table 3 in Valyavin et al. (2008)) of the strong–magnetic spot on the disc seem to have a similar tendency, shifted in phase by this value.

This phase shift was first observed by Wade et al. (2003) in their study of WD 1953–011 where they also estimated the "visibility" of the strong–magnetic area analyzing the Hα equivalent widths. This shift could be produced by the presence of some morphologic difference in the distribution of the field and photometric flux intensities within the corresponding spots. Although the origin of the shift could be artificial due to uncertainties in our simplifying assumption that the variation of equivalent widths of the Balmer line profiles is attributed to the strong–magnetic area only. The shift is, however, weak. And the general behaviour of all the observables related to the dark and strong–field magnetic areas exhibit a correlated behaviour suggesting their geometric relationship.

Taking all of the above into account, we suppose that the dark and magnetic spots are physically connected.

5 Discussion

We have presented new photometric and spectral observations of the magnetic white dwarf WD 1953–011. From these observations, and those previously published we have re–determined the star's rotation period, and studied the relationship between the brightness variation and the variation of the strong–magnetic spot projection. We find a new period of $P = 1.441788(6)$ days. This period is consistent with all the observables we employed, including those associated with the global magnetic field.

From a direct comparison of the phased photometric and spectroscopic observations we have found that the extremum of the photometric variations of the V–band flux, and the extremum of the varying projection of the magnetic spot to the line of sight are associated with each other with a possible small phase shift within the characteristic sizes of the spots.

An estimation of the photometric variation in terms of thermal inhomogeneity over the star's surface enables us to suggest that the variability comes from a low–temperature dark spot covering about 15–20% of the star's surface. The spot might have a temperature, characteristically lower than the mean by a factor of about 20%.

Due to these arguments, we suggest that the association between the dark spot and the strong–field area in WD 1953–011 is real, which leads to the fundamental problem related to the origin and evolution of the localized magnetic flux tubes in the isolated white dwarfs (see discussions in Brinkwoth et al., 2005; Valyavin et al., 2008). This idea, however, requires additional observational evidence, such as the presence of a secular drift of the tube which is still not established in WD 1953–011.

Acknowledgements. Our thanks to L. Ferrario, P. Maxted, and C. Brinkworth for providing the details of individual spectroscopic and photometric measurements of WD 1953–011. GAW acknowledges the Discovery Grant support from the Natural Sciences and Engineering Research Council of Canada. IH thanks the KFICST (grant 07–179). S. Plachinda acknowledge the support from the Ukrainian Fundamental Research State Fund (M/364) and the Austrian Science Fund (P17890). LFM and MA acknowledge the financial support from the UNAM via the PAPIIT grant IN114309. DS acknowledges financial support from Deutsche Forschungsgemeinschaft (DFG), Research Grant RE1664/7–1, and the FWF Lise Meitner grant Nr. M998–N16.

References

Brinkworth C. S., Marsh T. R., Morales–Rueda L., Maxted P. F. L., Burleigh M. R., Good S. A., 2005, MNRAS, 357, 333

Doroshenko V. T., Sergeev S. G., Pronik V. I., 2008, Astronomy Reports, 52, 442

Koester D., Dreizler S., Weidemann V., Allard N. F., 1998, A&A, 338, 612

Lafler J., Kinman T. D., 1965, ApJS, 11, 216

Levine S., Chakrabarty D., 1994, IA–UNAM, Technical Report, N. MU–94–04

Maxted P. F. L., Ferrario L., Marsh T. L., Wickramasinghe D. T., 2000, MNRAS, 315, L41

Parker E. N., 1979, "Cosmical magnetic fields", Oxford: Clarendon press

Valyavin G., Antonyuk K., Plachinda S., Clark D. M., Wade G. A., Fox Machado L., Alvarez M., Lopez J. M., Hiriart D., Han I., Jeon Y.–B., Bagnulo S., Zharikov S. V., Zurita C., Mujica R., Shulyak D., Burlakova T., 2011, ApJ, 734, 17

Valyavin G. G., Wade G. A., Bagnulo S., Szeifert T., Han I., Landstreet J. D., Burenkov A., 2008, ApJ, 683, 466

Wade G. A., Bagnulo S., Szeifert T., Brinkworth C., Marsh T., Landstreet J. D., Maxted P., 2003, ASP Conf. Ser., 307, 565